5074 *Biochemistry* **2010,** *49,* 5074–5081
DOI: 10.1021/bi100552d

BIOCHEMISTRY
including biophysical chemistry & molecular biology
Article

Class Pi Glutathione Transferase Unfolds via a Dimeric and Not Monomeric Intermediate: Functional Implications for an Unstable Monomer†

Samantha Gildenhuys, Louise A. Wallace, Jonathan P. Burke, David Balchin, Yasien Sayed, and Heini W. Dirr*

Protein Structure-Function Research Unit, School of Molecular and Cell Biology, University of the Witwatersrand, Johannesburg 2050, South Africa

Received April 12, 2010; Revised Manuscript Received May 18, 2010

ABSTRACT: Cytosolic class pi glutathione transferase P1-1 (GSTP1-1) is associated with drug resistance and proliferative pathways because of its catalytic detoxification properties and ability to bind and regulate protein kinases. The native wild-type protein is homodimeric, and whereas the dimeric structure is required for catalytic functionality, a monomeric and not dimeric form of class pi GST is reported to mediate its interaction with and inhibit the activity of the pro-apoptotic enzyme c-Jun N-terminal kinase (JNK) [Adler, V., et al. (1999) *EMBO J. 18*, 1321−1334]. Thus, the existence of a stable monomeric form of wild-type class pi GST appears to have physiological relevance. However, there are conflicting accounts of the subunit's intrinsic stability since it has been reported to be either unstable [Dirr, H., and Reinemer, P. (1991) *Biochem. Biophys. Res. Commun. 180*, 294−300] or stable [Aceto, A., et al. (1992) *Biochem. J. 285*, 241−245]. In this study, the conformational stability of GSTP1-1 was re-examined by equilibrium folding and unfolding kinetics experiments. The data do not demonstrate the existence of a stable monomer but that unfolding of hGSTP1-1 proceeds via an inactive, nativelike dimeric intermediate in which the highly dynamic helix 2 is unfolded. Furthermore, molecular modeling results indicate that a dimeric GSTP1-1 can bind JNK. According to the available evidence with regard to the stability of the monomeric and dimeric forms of GSTP1-1 and the modality of the GST−JNK interaction, formation of a complex between GSTP1-1 and JNK most likely involves the dimeric form of the GST and not its monomer as is commonly reported.

Glutathione *S*-transferases (GSTs,[1] EC 2.5.1.18) make up a large superfamily of multifunctional proteins involved in catalytic detoxification reactions and in regulation of signaling pathways via protein−protein interactions (reviewed in ref *1*). All cytosolic GSTs are dimeric and share a common fold, with each subunit consisting of two distinct domains (for example, see Figure 1). A dimeric structure and its conformational stability and dynamics have important implications for function. Assembly of a GST dimer is critical for catalysis since both subunits contribute to binding the physiological substrate glutathione (GSH) at the active site on each subunit (*2*). Quaternary interactions also contribute substantially toward maintaining the functional conformation of the active site (*3*−*9*), the cooperative behavior between subunits (*7*, *10*, *11*), and the conformational stability (*12*−*22*) and dynamics (*23*, *24*) of the individual subunits. Furthermore, a recent study of the dimer−monomer equilibrium of wild-type GSTs demonstrated that the dimeric structure is highly stable in solution, displaying K_d values in or below the nanomolar range (*11*).

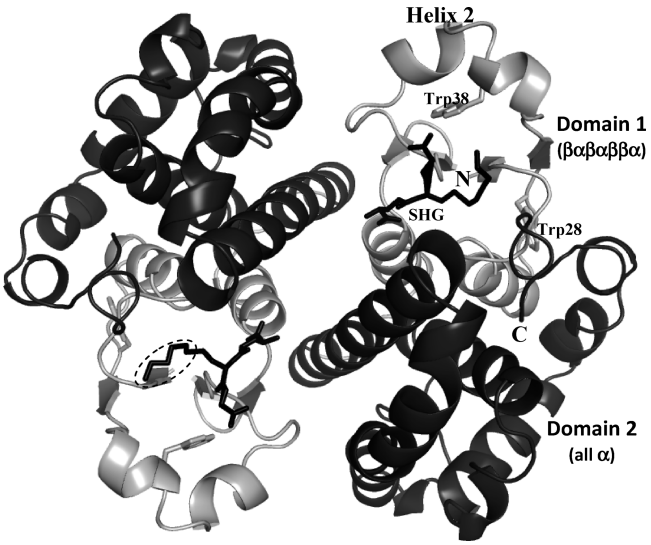

FIGURE 1: Ribbon diagram of human GSTP1-1 in complex with *S*-hexylglutathione viewed down the 2-fold axis [Protein Data Bank entry 1GSS (*38*)]. Domain 1 and domain 2 are colored light and dark gray, respectively. Stick models of the two tryptophan residues in domain 1 are colored gray and the stick models for *S*-hexylglutathione (SHG) black. The oval indicates the hexyl moiety of the ligand. The N- and C-termini are indicated. The model was generated with PyMOL (http://pymol.sourceforge.net/).

Class pi glutathione transferase P1-1 (GSTP1-1), which is overexpressed in many tumors, is implicated in the development of anticancer drug resistance and in tumorigenesis via the protein's catalytic detoxification and noncatalytic binding functionalities

†This work was supported by the University of the Witwatersrand, the South African National Research Foundation (Grant 205359), the South African Research Chairs Initiative of the Department of Science and Technology, and the National Research Foundation (Grant 64788).

*To whom correspondence should be addressed. Telephone: +27 11 7176352. Fax: +27 11 7176351. E-mail: heinrich.dirr@wits.ac.za.

[1]Abbreviations: ANS, 8-anilinonaphthalene-1-sulfonate; CD, circular dichroism; CDNB, 1-chloro-2,4-dinitrobenzene; C_m, midpoint of an unfolding transition at which 50% of the protein molecules are denatured; DTT, 1,4-dithiothreitol; GSH, glutathione; GSO_3^-, glutathione sulfonate; GST, glutathione *S*-transferase; hGSTP1-1, human class pi GST with two type 1 subunits; $\Delta G(H_2O)$, free energy change in the absence of denaturant; HMQC, heteronuclear multiple-quantum coherence; JNK, c-Jun N-terminal kinase; PDB, Protein Data Bank.

 Published on Web 05/19/2010

(reviewed in refs *25* and *26*). Whereas the dimeric structure (Figure 1) is essential for catalytic activity (see ref *11*), a stable monomeric form of the wild-type class pi GST is thought to exist and is reported to interact with and inhibit the pro-apoptotic enzyme c-Jun N-terminal kinase (JNK), thereby enhancing the proliferative nature of cancer cells (*27*). Thus, the thermodynamic stability of the wild-type class pi subunit in the absence of quaternary interactions appears to have physiological relevance. However, there are conflicting conclusions regarding the intrinsic stability of the class pi subunit; it has been reported to be either unstable (*12*) or stable (*13*).

In this study, the equilibrium folding behavior and unfolding kinetics of hGSTP1-1 were investigated to reassess the question of the intrinsic stability of the individual subunits in the absence of a dimer interface. Molecular docking was also performed to establish the capability of dimeric GSTP1-1 to bind JNK. Overall, the data demonstrate the thermodynamic instability of the class pi monomer and that the dimer can bind JNK. These findings have implications for the reported existence and functional roles of a stable, folded monomeric class pi GST.

EXPERIMENTAL PROCEDURES

Materials. Ultrapure urea and DTT were purchased from ICN Biomedicals Inc. (Aurora, OH). Reduced glutathione and glutathione sulfonate were obtained from Sigma. All other reagents were of analytical grade.

Expression and Purification of hGSTP1-1. The plasmid encoding the cDNA for hGSTP1-1 was a gift from R. T. Baker (The Australian National University, Canberra, Australia). hGSTP1-1 was overexpressed in TG1 *Escherichia coli* cells containing the pRB307-pBR173 plasmids (*28*). In this ubiquitin fusion/cotranslational cleavage system, hGSTP1-1 is expressed in high yields as a fusion protein with ubiquitin. The latter is cleaved from the N-terminus of the GST by a protease expressed by the pBR173 plasmid. hGSTP1-1 was purified using *S*-hexylglutathione affinity chromatography and eluted using 50 mM glycine-NaOH (pH 10.0) containing 2 mM DTT. The high pH enables elution of the apo form of the protein without the use of free *S*-hexylglutathione. Immediately following elution, the pH of the protein-containing solution was adjusted to pH 6.5 using 0.5 M NaH_2PO_4. The protein was buffer-exchanged by means of dialysis into 20 mM sodium phosphate buffer (pH 6.5) containing 0.1 M NaCl, 1 mM EDTA, and 2 mM DTT. The structural homogeneity was assessed using SDS−PAGE and size exclusion HPLC, and no uncleaved fusion protein was found to be present. The activity of the protein was assessed using the standard CDNB conjugating assay as described previously (*29*). The concentration of the pure protein was determined using a molar extinction coefficient of 55320 M^{-1} cm^{-1} at 280 nm.

Unfolding Studies. Equilibrium unfolding studies of hGSTP1-1 [0.5−5 μM in 20 mM phosphate buffer (pH 6.5) containing 100 mM NaCl, 0.1 mM EDTA, and 2 mM DTT] were performed at 20 °C with 0−8 M urea as described previously (*17*). Structural changes upon unfolding and refolding were assessed by far-UV CD and tryptophan fluorescence (excitation at 295 nm). Rayleigh scattering (excitation and emission wavelengths set at 295 nm) was monitored to ensure the absence of aggregation during unfolding and refolding. Values for the conformational stability parameters, $\Delta G(H_2O)$ (free energy of unfolding in the absence of urea) and m value (cooperativity factor), were obtained by nonlinear least-squares regression analysis of the equilibrium unfolding data using a two-state model (*17*, *30*).

Unfolding kinetics were measured at 20 °C by fluorescence using a stopped-flow mixing device with a dead time of 2 ms (SX-18 MV, Applied Photophysics). The excitation and emission path lengths were 10 and 2 mm, respectively. Excitation was at 290 nm and the emission monitored using a 320 nm cutoff filter. hGSTP1-1, initially at 6 μM in buffer, was diluted 6-fold (1:5) with urea in buffer to give a final protein concentration of 1 μM in 5−7.5 M urea. Kinetic traces were analyzed and fitted by the nonlinear least-squares method using the Applied Photophysics software version 4.47. Residual plots were used to assess the quality of the fits.

Size Exclusion HPLC. The retention times of 1 μM hGSTP1-1 in the absence and presence of urea (0, 4.2, or 5.2 M) were measured by analytical size exclusion HPLC at 20 °C in 20 mM sodium phosphate buffer (pH 6.5), 0.1 M NaCl, 1 mM EDTA, 0.5 mM TCEP, and 0.02% sodium azide using a Tosoh Bioscience 2000swxl SEC-HPLC column (Tosoh Bioscience). The column was pre-equilibrated with buffer with or without urea and the protein eluted with the same buffer. Elution profiles were recorded by fluorescence with excitation and emission wavelengths set at 280 and 335 nm, respectively.

Isothermal Titration Calorimetry. Calorimetric studies were conducted at 20 °C using a VP-ITC MicroCalorimeter from MicroCal Inc. Purified hGSTP1-1 was passed through a Sephadex-G25 column and dialyzed extensively against 20 mM sodium phosphate buffer (pH 6.5) containing 0.1 M NaCl, 1 mM EDTA, 0.5 mM TCEP, and 0.02% sodium azide. The ligand, GSO_3^-, was prepared in the final dialysate buffer. The protein concentration was determined at 280 nm as described above and corrected for any light scattering effects. A solution of 2 mM GSO_3^- was injected into the ITC sample cell that contained 82 μM hGSTP1-1 (subunit concentration). GSO_3^- was added until saturation was achieved. To correct for the heats of dilution, control experiments were performed by making identical injections of ligand into a buffer solution without protein. The heat of dilution was subtracted from the experimental raw data giving the corrected heats of the binding reaction. The raw data obtained from the calorimetric experiments were collected and integrated using ORIGIN version 5 (MicroCal Inc.).

Molecular Docking of GSTP1-1 and JNK. JNK1 [PDB entry 3ELJ (*31*)] was docked onto the structure of GSTP1-1 [PDB entry 16GS (*32*)] using ZDOCK (*33*), ZRANK (*34*), and RDOCK (*35*) within the Accelrys Discovery Studio suite. The N-terminal domain of JNK1 (residues 1−206) was not defined for docking on the basis of the findings of Wang et al. indicating the involvement of the C-terminal domain in binding the GST (*36*). The proteins were first docked using ZDOCK on the basis of shape complementarity and then reranked using ZRANK on the basis of more detailed electrostatics, van der Waals, and desolvation energy calculations. The top 30 scoring poses obtained from ZRANK were refined using RDOCK based on CHARMM-based energy minimization criteria (*37*). All the top scoring clusters displayed a similar orientation, with the GST dimer interface uninvolved in the protein−protein interaction. The top scoring pose from this procedure is reported here.

RESULTS

Probes for Monitoring Structural Changes during Unfolding. Each subunit in hGSTP1-1 consists of two nonidentical

domains (Figure 1). Domain 1 (residues 1−76) contains the two tryptophan residues (Trp28 in strand 2 and Trp38 in helix 2) and has 37% of the total secondary structure (31 residues in α helices and 18 residues in β strands). Domain 2 (residues 83−209) has no tryptophans but has 63% of the total secondary structure (83 residues in α helices and none in β strands). hGSTP1-1 displays a far-UV CD spectrum with ellipticity minima at 208 and 222 nm that is typical of a predominantly α-helical protein (data not shown). Since most of the protein's helical structure is found in domain 2, the signal measured at 222 nm during unfolding will report primarily on structural changes in this domain. Fluorescence measurements, on the other hand, will follow structural changes around the two tryptophan residues in domain 1. Should the two domains unfold independently of one another, the unfolding of domain 2 will be invisible to fluorescence measurements. The maximum emission wavelength of folded hGSTP1-1 is 335 nm, consistent with the partial burial of both tryptophans (*38*), shifts to 355 nm, and is accompanied by an increase in fluorescence intensity when hGSTP1-1 unfolds (data not shown).

Enzyme activity and 8-anilinonaphthalene-1-sulfonate (ANS) binding were also used to follow unfolding by detecting structural changes at or near the active site. The active site on each subunit consists of two adjacent subsites: a G-site on domain 1 for GSH and an H-site along the domain interface for electrophilic substrates (Figure 1). While native GSTs have been shown to bind the amphipathic dye ANS at or near the active site (*39*, *40*), the dye has also been used to detect the presence of hydrophobic patches that become exposed during unfolding (*16*, *19*, *21*, *41*). The emission spectrum of ANS shifts from 530 nm in water to 480 nm when ANS is bound to hGSTP1-1 which is accompanied by a large increase in emission intensity. The dye does not bind unfolded GST, and binding does not affect the stability of GSTs (*42*, *43*).

Equilibrium Unfolding of Apo and GSO_3^--Complexed hGSTP1-1. The urea-induced unfolding reaction of homodimeric hGSTP1-1 was studied at pH 6.5 and 20 °C and monitored with a variety of structural and functional probes (see above). The coincidence of the unfolding and refolding curves for a specific spectroscopic probe (Figure S1 of the Supporting Information) indicates thermodynamic reversibility (> 95%) and the absence of unfolding−refolding hysteresis, a prerequisite for establishing the thermodynamics of the unfolding process.

The equilibrium unfolding data for apo hGSTP1-1 (Figure 2A) show that the CD and fluorescence unfolding curves do not coincide, suggesting that equilibrium unfolding and refolding are not two-state processes. While the CD curve displays a monophasic transition ranging between 3 and 5.2 M urea, changes in tryptophan fluorescence begin to occur at lower urea concentrations (~1−1.5 M urea) and coincide with the CD curve only at higher urea concentrations. Furthermore, enzyme activity and the level of ANS binding begin to decrease simultaneously from ~1.5 M urea, and both appear to follow the change in fluorescence during denaturation. It is noteworthy that there is no increase in the level of ANS binding at low denaturant concentrations as observed for certain GSTs and other dimeric proteins which first dissociate to structured monomers with exposed hydrophobic patches prior to complete unfolding (*16*, *19*, *21*, *41*). The ANS binding behavior of hGSTP1-1 reflects that of GSTs which have been shown to unfold from a dimeric state to denatured monomers (*14*, *17*). Together, the data obtained from the various probes used to monitor unfolding (see above) indicate that domain 1, or part thereof, is less stable

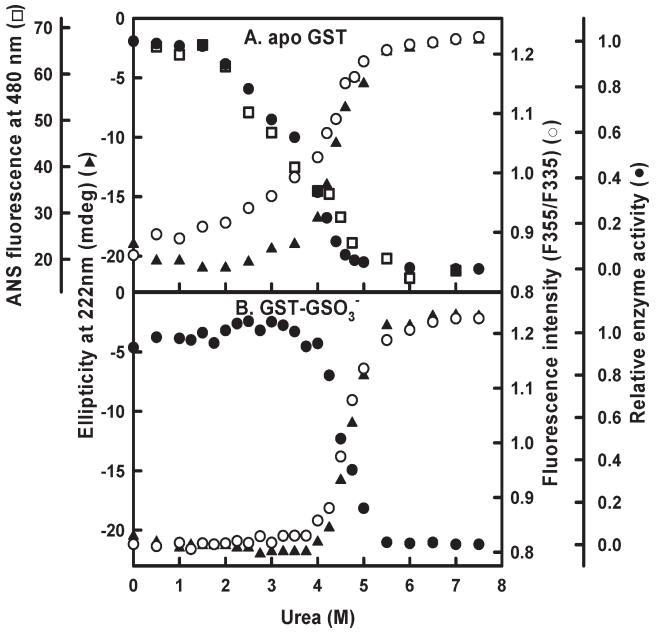

FIGURE 2: Urea-induced unfolding curves for hGSTP1-1 in its apo form (A) and in a complex with GSO_3^- (B) monitored by far-UV CD (▲), tryptophan fluorescence (○), enzyme activity (●), and ANS binding (□). The hGSTP1-1 concentration was 2 μM in 20 mM phosphate buffer (pH 6.5) containing 100 mM NaCl, 0.1 mM EDTA, and 2 mM DTT. The concentrations of ANS and GSO_3^- were 200 and 150 μM, respectively. F_{355}/F_{335} is the ratio of the fluorescence intensity at 355 nm (unfolded protein) to that at 335 nm (folded protein) with excitation at 295 nm. The relative enzyme activity is the activity relative to that in the absence of urea. ANS fluorescence was measured at 480 nm with excitation at 390 nm.

than domain 2. Domain 1 contains both tryptophan residues in hGSTP1-1 (Figure 1), and ~50% of the change in tryptophan fluorescence observed during unfolding occurs at low urea concentrations (1−3.8 M) where no significant change in secondary structure occurs (Figure 2A). However, at higher urea concentrations, the remaining fluorescence change occurs with the disruption of the secondary structure, suggesting that the unfolding of domain 1 is not entirely independent of domain 2, consistent with an extensive interface between the domains.

Helix 2, a highly dynamic structure in apo hGSTP1-1 (*32*, *44*), is located at the active site where it forms a major part of the G-site (Figure 1), and Trp38 in helix 2 has been used to probe the dynamics of the helix (*45*). Since helix 2 becomes stabilized by the binding of G-site ligands (*44*), GSO_3^- [K_d = 2.2 μM at 20 °C as determined by ITC (see Figure S2 of the Supporting Information)] was used to establish the involvement of helix 2 in the unfolding of hGSTP1-1. While the binding of GSO_3^- appears to have a small stabilizing effect on the secondary structure, it produces significant changes in the unfolding of the protein when monitored by fluorescence and enzyme activity (Figure 2B). The pretransition region of the CD curve for the apo enzyme displays a slight increase between 1 and 4 M urea (Figure 2A) that becomes flatter for the GST·GSO_3^- complex (Figure 2B), suggesting that the ligand might be stabilizing some (~7−10% based on the observed signal changes) of the total helical structure without affecting the major unfolding transition. This value corresponds to that of helix 2 which makes up 8% of the total helical content of hGSTP1-1. The initial increase in tryptophan fluorescence observed with the apo enzyme at low urea concentrations (Figure 2A) is now absent for the GST·GSO_3^- complex, and the entire fluorescence unfolding

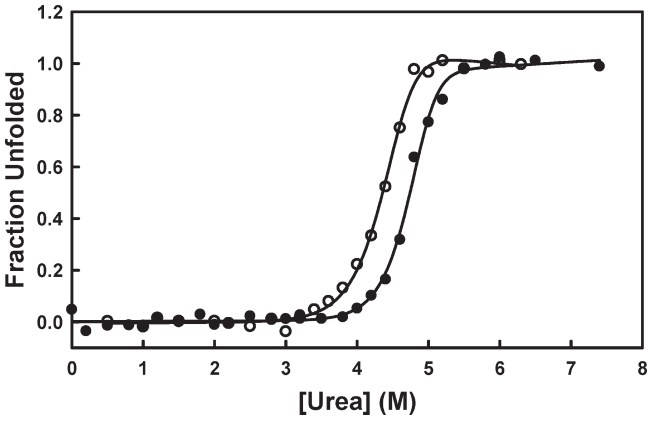

FIGURE 3: Protein concentration dependence of unfolding. Unfolding transitions for 0.5 μM (empty symbols) and 5 μM (filled symbols) hGSTP1-1 monitored by far-UV CD. The solid lines are the nonlinear regression fits to the data based on a two-state $N_2 \leftrightarrow 2U$ model. The parameters obtained for 0.5 μM hGSTP1-1 are as follows: $\Delta G(H_2O) = 24.6 \pm 1.3$ kcal/mol, and $m = 3.7 \pm 0.3$ kcal mol^{-1} M^{-1}. The parameters obtained for 5 μM hGSTP1-1 are as follows: $\Delta G(H_2O) = 26.9 \pm 1.1$ kcal/mol, and $m = 4.2 \pm 0.2$ kcal mol^{-1} M^{-1}.

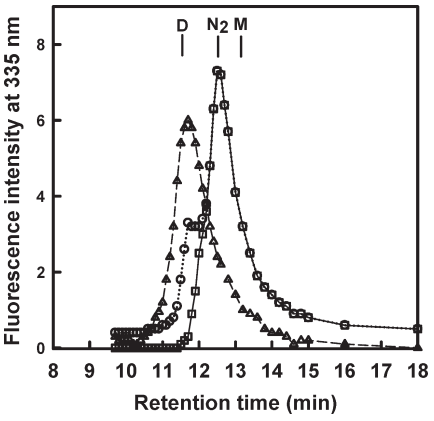

FIGURE 4: Size exclusion HPLC of hGSTP1-1 in the absence and presence of urea. hGSTP1-1 (1 μM) was incubated with urea and applied to and eluted from a 2000swxl SEC-HPLC column preequilibrated with the same concentration of urea: 0 (□), 4.2 (○), and 5.2 M (△). N_2 and D indicate the retention times for dimeric and denatured hGSTP1-1, respectively. M indicates the expected retention time for a structured monomeric hGSTP1.

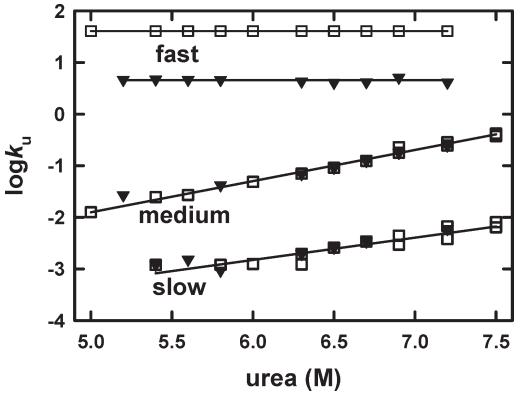

FIGURE 5: Urea dependence of the unfolding rate constants, k_u, of apo hGSTP1-1 (□) and the hGSTP1-1·GSO_3^- complex (▼). All phases were detected using tryptophan fluorescence and are designated as fast, medium, and slow on the basis of the time scale of the events. The hGSTP1-1 concentration was 1 μM in 20 mM phosphate buffer (pH 6.5) containing 100 mM NaCl, 0.1 mM EDTA, and 2 mM DTT. The concentration of GSO_3^- was 150 μM. The solid lines are linear regression fits to the data.

curve overlays well with the far-UV CD curve (Figure 2B). The enzyme activity curve is also shifted to higher urea concentrations where it coincides with both spectroscopic curves (Figure 2B). Although GSO_3^- is a competitive inhibitor ($IC_{50} = 28$ μM) (*46*), its concentration was significantly reduced (0.4 μM) by dilution during the enzyme assays. These results demonstrate the involvement of helix 2 in the structural changes of the apo protein at low urea concentrations.

Given the observed decrease in enzyme activity and changes in tryptophan fluorescence of the apo enzyme at low urea concentrations prior to the disruption of secondary structure (Figure 2A), it is possible that the dimeric protein first dissociates to two structured monomers before unfolding completely, as observed for other GSTs (*13*, *16*, *19*, *21*, *41*). This possibility was explored by determining the protein concentration dependence of unfolding. Should the activity and fluorescence data at low urea concentrations indicate dissociation to structured monomers, then the CD data should report the unfolding of these monomers, which, according to the law of mass action, should be independent of protein concentration. The unfolding curves shown in Figure 3, however, demonstrate that the entire unfolding transition shifts to higher urea concentrations with an increase in protein concentration due to a change in molecularity upon equilibrium unfolding, as expected for a dimeric protein as it unfolds to and refolds from two denatured monomers in a two-state process (*47*, *48*). Furthermore, the experimental *m* values obtained from the data in Figure 3 compare favorably with the expected change in solvent-accessible surface area between the native dimer and denatured monomers of hGSTP1-1 (predicted *m* value of 4.5 kcal mol^{-1} M^{-1}) (*49*). The lower experimental *m* values for the CD data in Figure 3 could be due to an already unfolded helix 2 in the partially unfolded dimeric protein at the beginning of the unfolding transition. On the basis of its size, a fully folded helix 2 could contribute ~0.5 kcal mol^{-1} M^{-1} to the *m* value of dimeric hGSTP1-1.

Size exclusion HPLC has also been used to demonstrate the absence or presence of stable monomeric intermediates in the unfolding of GSTs (*13*−*15*, *19*, *24*). The elution profiles obtained for hGSTP1-1 in the absence and presence of urea indicate that only two species are present during unfolding: one corresponding to dimeric protein and the other to denatured monomeric hGSTP1, both of which are present at 4.2 M urea (Figure 4). There is no indication of the presence of a folded, monomeric form of the protein, consistent with the data described above.

Unfolding Kinetics. The unfolding of apo hGSTP1-1 in 5−7.5 M urea, measured by tryptophan fluorescence, follows triphasic kinetics (Figure S3 of the Supporting Information). The first (fast) and third (slow) phases exhibit positive amplitude changes, whereas the second (medium) phase displays a negative amplitude change. No burst phase occurs within the dead time, and the initial and final amplitudes are as predicted by equilibrium experiments. The logarithms of the rate constants for the medium and slow phases increase linearly with urea concentration, while those for the fast phase are independent of urea (Figure 5; empty symbols for the apo form). The unfolding data were fit to the linear equation

$$\log k_u = \log k_u(H_2O) + (m_u^{\ddagger}/2.303RT)[\text{urea}]$$

where k_u is the rate constant for unfolding at a urea concentration, $k_u(H_2O)$ is the rate constant of unfolding in the absence of

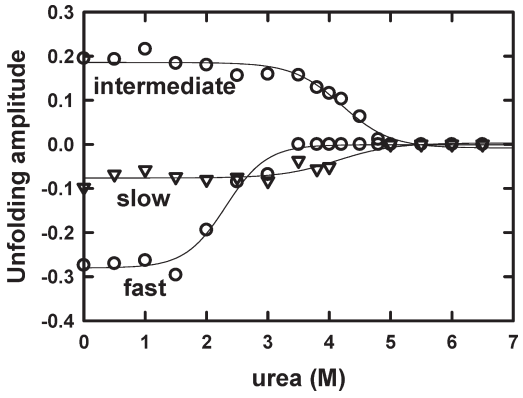

FIGURE 6: Initial conditions test for the unfolding kinetics of apo hGSTP1-1. The protein was preincubated in urea at the concentrations shown (0−6.5 M) and the unfolding kinetics measured when the urea concentration was adjusted to 6.5 M. The final protein concentration was 1 μM in 20 mM phosphate buffer (pH 6.5) containing 100 mM NaCl, 0.1 mM EDTA, and 2 mM DTT. The amplitude changes for the three unfolding phases are as indicated, and the solid lines are nonlinear regression fits to the data.

urea, and $m_u^{\ddagger}$ is the m value for the activation process from the native state to the transition state. The fits to the unfolding data in Figure 5 yield $k_u(H_2O)$ values of 40.7, 1.2×10^{-5}, and 3.8×10^{-6} s^{-1} for the fast, medium, and slow phases, respectively, and $m_u^{\ddagger}$ values of 0, 0.8, and 0.6 kcal mol^{-1} M^{-1} for the fast, medium, and slow phases, respectively. The high $k_u(H_2O)$ value for and urea independence of the fast phase indicate the involvement of a highly dynamic and unstable structural element that undergoes a small change in the solvent-accessible surface area during this unfolding event. The $m_u^{\ddagger}$ values are much smaller than the m values obtained from the equilibrium studies [3.7−4.2 kcal mol^{-1} M^{-1} (Figure 3)], suggesting that the rate-limiting transition states for these unfolding events resemble more closely the native state than the unfolded state. The absence of "rollovers" (i.e., nonlinear dependencies of log k_u on urea concentration) in Figure 5 indicates that unfolding does not proceed via a high-energy intermediate such as a monomeric intermediate.

Because three kinetic unfolding phases are observed, an initial conditions test was performed to establish whether they occur sequentially or in parallel (*50*). Different initial urea concentrations were used (0−6.5 M), while the final urea concentration was kept constant at 6.5 M. The dependence of the rate constants and amplitudes of unfolding reactions on the initial urea concentrations were determined by relying on the fact that rate constants depend only on the final conditions while amplitudes depend on both the initial and final conditions (*50*). Unfolding kinetics is triphasic at initial urea concentrations of < 3.5 M but becomes biphasic at higher concentrations, as indicated by the amplitudes in Figure 6. From 1.5 to 3.5 M urea, the amplitude of the fast phase diminishes to zero with a midpoint at ~2.5 M urea, corresponding to the fluorescence changes observed during the equilibrium unfolding of apo hGSTP1-1 (Figure 2A). The amplitudes of the medium and slow phases simultaneously reduce to zero at ~5.5 M urea, displaying midpoints at ~4.3 M urea which is close to the midpoint observed for the major unfolding transition in equilibrium studies (Figure 2A). The rate constants resemble those for the corresponding phases when the initial concentration of urea was 0 M and the final concentration was 6.5 M (data not shown). The relative amplitudes at an initial urea concentration of 0 M are 48.3, 34.4, and 17.3% for the fast, medium, and slow phases, respectively. Since these amplitudes represent the fraction of molecules present at the beginning of the reaction (*51*), the simultaneous presence of three unfolding phases indicates that the three unfolding reactions occur independently and, thus, run in parallel (*50*).

Because unfolding of helix 2 was established in equilibrium unfolding studies of hGSTP1-1 using GSO_3^-, the G-site ligand was also used to establish if any of the kinetics phases involve the unfolding of the helix. While the rates of the medium and slow unfolding phases were essentially unchanged by the binding of GSO_3^- to hGSTP1-1, the ligand reduced the rate of the fast phase by ~8-fold [Figure 5 (▼)], yielding a $k_u(H_2O)$ of 5.2 s^{-1}. These results together with those obtained from the initial conditions test for the fast phase (Figure 6) provide compelling evidence that the fast phase represents the unfolding kinetics of helix 2. The occurrence of the two other independent unfolding phases (i.e., medium and slow), as indicated by the initial conditions test, suggests global unfolding of two native state forms of hGSTP1-1. Native state heterogeneity has also been reported for the monomeric GST homologue Grx-2 (*52*). The origin of the heterogeneity in both proteins is, however, unclear at present. Taken together, the kinetics data do not indicate a sequential pathway in which dimeric hGSTP1-1 first dissociates to folded monomers followed by their unfolding.

DISCUSSION

Unfolding Mechanism. Monomeric Class Pi GST Is Thermodynamically Unstable. Protein−protein interfaces can have a profound effect on the stability and unfolding mechanism of proteins (*48*, *53*). Dimeric GSTs possess a complex canonical structure (Figure 1), its assembly involving interactions at the subunit interface and at the domain interface. Interdomain interactions are extensive and contribute substantially to the stability of the individual GST subunits (*54*), and studies with both dimeric and monomeric GSTs and GST-like proteins indicate that the two domains do not unfold independently but that they behave as a single cooperative unit (*14*−*17*, *19*, *52*, *55*). The effects of interactions across the GST dimer interface do, however, give rise to complex unfolding processes ranging from a two-state transition involving only native dimer and unfolded monomers (*15*, *17*, *19*) to multistate transitions that include thermodynamically stable monomeric and/or dimeric intermediates (*16*, *18*−*20*, *22*, *41*). There are, nevertheless, conflicting reports regarding the intrinsic stability of the class pi subunit in the absence of quaternary interactions. The porcine subunit is reported to be unstable (*12*, *14*), whereas the human subunit is reported to be inactive but stable (*13*). Given the high degree of sequence identity (84%) and conserved three-dimensional structures of these class pi orthologues (*38*, *56*), it would be surprising if they did not share a conserved unfolding−refolding reaction (*57*). It was proposed that the loss of enzyme activity of the human enzyme was due to the dissociation of the native dimer to two structured but inactive monomers (*13*). However, the unfolding transition monitored by activity exhibited little dependence upon protein concentration, in contrast to what would be expected for a dimer−monomer equilibrium (*47*, *48*), and the protein concentration dependence of the transitions monitored by spectroscopic probes was not reported. What neither of the studies with class pi GST considered were the dynamic nature and potentially inherent instability of helix 2, a structural element that forms an integral part of the active site (*38*, *56*).

In this study, we re-examined the unfolding of human GSTP1-1 and present compelling evidence from equilibrium and kinetics experiments that helix 2 unfolds at low concentrations of urea prior to global unfolding resulting in an inactive, dimeric intermediate with no evidence of a stable monomeric intermediate. On the basis of our data (Figures 2−4), we propose the following three-state model for the equilibrium unfolding of apo class pi GST:

$$N_2(\alpha2)_{f,m} \leftrightarrow N_2(\alpha2)_u \leftrightarrow 2U$$

where N_2 is the native dimer with helix 2 (α2) in a folded and mobile conformation (subscripts f and m, respectively) or unfolded (subscript u) and U is the unfolded monomer. At 20 °C, the temperature at which the unfolding studies were performed, or at lower temperatures, helix 2 is predominantly folded but mobile (*44*). During the first unfolding reaction which occurs at low urea concentrations, the native dimeric enzyme forms a partially denatured dimeric intermediate in which helix 2 is unfolded. The unfolding of helix 2 results in the disruption of the tertiary environment of both Trp38 and the active site, consequently leading to a loss of both catalytic and ligandin (ANS binding) functions. The second reaction which is protein concentration-dependent represents the global unfolding of the dimeric intermediate at higher urea concentrations via a highly cooperative two-state process in which dissociation of the dimer and its unfolding are tightly coupled events. The concerted dissociation−unfolding process of hGSTP1-1 is in accord with that observed for the porcine class pi orthologue (*12*, *14*) and other GSTs (*15*, *17*, *19*) whose individual subunits are thermodynamically unstable in the absence of quaternary interactions.

Ligand binding to the class pi G-site occurs via an induced fit binding mechanism during which helix 2 adopts a less dynamic conformation (*32*, *58*), with little effect on the stability of the global dimeric structure (*59*). Our data (Figure 2) indicate that unfolding of the hGSTP1-1·GSO_3^- complex is a highly cooperative two-state process in that the bound G-site inhibitor stabilizes helix 2 by inducing its localization (immobilization) at the active site, thus significantly reducing the population of $N_2(\alpha2)_u$:

$$N_2(\alpha2)_{f,l} \cdot GSO_3^- \leftrightarrow 2U$$

where helix 2 (α2) is in a folded and localized conformation (subscripts f and l, respectively). Stabilization of the corresponding helix 2 in class sigma GSTS1-1 by G-site ligands has also been reported (*16*).

The unfolding kinetics data (Figures 5 and 6) indicate a more complex unfolding mechanism. Unfolding kinetics are characterized by three events: a fast phase, a medium phase, and a slow phase, none of which appear to involve a monomeric intermediate. We propose the following parallel kinetics pathway for the unfolding of apo class pi GST:

$$N_2'(\alpha2)_{f,m} \xrightarrow{\text{fast}} N_2'(\alpha2)_u \xrightarrow{\text{medium (34\%)}} 2U$$

$$N_2''(\alpha2)_{f,m} \xrightarrow{\text{fast}} N_2''(\alpha2)_u \xrightarrow{\text{slow (17\%)}} 2U$$

where $N_2'(\alpha2)_{f,m}$ and $N_2''(\alpha2)_{f,m}$ represent native state heterogeneity in hGSTP1-1 in which helix 2 is folded and mobile, the fast phase represents the unfolding of helix 2 in each native state yielding dimeric intermediates with unfolded helix 2 [$N_2'(\alpha2)_u$ and $N_2''(\alpha2)_u$], and the medium and slow phases represent the global unfolding of these dimeric intermediates to unfolded protein (U). The values in parentheses are the relative populations for the medium and slow phases. The relative population for the fast phase (∼48%) is proposed to feed into the medium and slow phases as shown. Whereas the level of unfolding of helix 2 is reduced significantly (∼8-fold) by the binding of GSO_3^- to the G-site, the unfolding kinetics of the dimeric intermediates are not affected, consistent with helix 2 not impacting the global stability of GSTP1-1.

Functional Implications of an Unstable Class Pi Monomer. Class pi GST is a prevalent cytosolic enzyme expressed at high levels in cancer cells and contributes, through its catalytic and noncatalytic functions, to the proliferative nature of tumors (*25*, *26*). GST is reported to suppress apoptosis and promote proliferation by binding to and inhibiting the activity of the pro-apoptotic protein c-Jun N-terminal kinase (JNK), and it is a structured monomeric and not dimeric form of the GST that initiates and mediates this protein−protein interaction (*27*). However, when considering the thermodynamic instability of the monomer (this study) and a K_d of ≤20 pM for the class pi homodimer (*11*), it is unclear from the study by Adler et al. how it was possible to purify a monomeric form of the wild-type enzyme and how its spontaneous dimerization was prevented. Furthermore, the concentrations of GSTP1-1 used to characterize the GST−JNK interaction (*36*) would certainly favor a predominantly dimeric form of the GST given the K_d of the dimer. Our molecular docking results demonstrate the capability of dimeric GSTP1-1 to form a complex with JNK1, with a JNK bound to each subunit of the GST (Figure S4 of the Supporting Information). The interfaces between the two binding partners are far removed from the GST dimer interface and involve protein segments previously implicated in complex formation, namely, the C-terminal region of domain 2 of GSTP1-1 and the C-terminal domain of JNK1 (*36*, *60*). Therefore, according to the available evidence regarding the stability of the monomeric and dimeric forms of GSTP1-1 and the modality of the GST−JNK interaction, the interaction between GSTP1-1 and JNK most likely involves the dimeric form of the GST and not its monomer as is commonly reported.

Furthermore, class pi GST has been reported to form a heterodimer with 1-cysteine peroxiredoxin (Prx) which involves a monomer from each protein (*61*−*63*). In the proposed GST−Prx complex, the quaternary interactions between the monomers in the native homodimers are replaced by GST−Prx interactions that could stabilize the individual monomeric structures.

SUPPORTING INFORMATION AVAILABLE

Four figures as described in the text. This material is available free of charge via the Internet at http://pubs.acs.org.

REFERENCES

1. Sheehan, D., Meade, G., Foley, V. M., and Dowd, C. A. (2001) Structure, function and evolution of glutathione transferases: Implications for classification of non-mammalian members of an ancient enzyme superfamily. *Biochem. J. 360*, 1–16.
2. Dirr, H., Reinemer, P., and Huber, R. (1994) X-ray crystal structures of cytosolic glutathione S-transferases. Implications for protein architecture, substrate recognition and catalytic function. *Eur. J. Biochem. 220*, 645–661.

3. Hornby, J. A., Codreanu, S. G., Armstrong, R. N., and Dirr, H. W. (2002) Molecular recognition at the dimer interface of a class mu glutathione transferase: Role of a hydrophobic interaction motif in dimer stability and protein function. *Biochemistry 41*, 14238–14247.
4. Sayed, Y., Wallace, L. A., and Dirr, H. W. (2000) The hydrophobic lock-and-key intersubunit motif of glutathione transferase A1-1: Implications for catalysis, ligandin function and stability. *FEBS Lett. 465*, 169–172.
5. Stenberg, G., Abdalla, A. M., and Mannervik, B. (2000) Tyrosine 50 at the subunit interface of dimeric human glutathione transferase P1-1 is a structural key residue for modulating protein stability and catalytic function. *Biochem. Biophys. Res. Commun. 271*, 59–63.
6. Vargo, M. A., Nguyen, L., and Colman, R. F. (2004) Subunit interface residues of glutathione S-transferase A1-1 that are important in the monomer-dimer equilibrium. *Biochemistry 43*, 3327–3335.
7. Wongsantichon, J., and Ketterman, A. J. (2006) An intersubunit lock-and-key 'clasp' motif in the dimer interface of delta class glutathione transferase. *Biochem. J. 394*, 135–144.
8. Piromjitpong, J., Wongsantichon, J., and Ketterman, A. J. (2007) Differences in the subunit interface residues of alternatively spliced glutathione transferases affects catalytic and structural functions. *Biochem. J. 401*, 635–644.
9. Huang, Y. C., Misquitta, S., Blond, S. Y., Adams, E., and Colman, R. F. (2008) Catalytically active monomer of glutathione S-transferase pi and key residues involved in the electrostatic interaction between subunits. *J. Biol. Chem. 283*, 32880–32888.
10. Caccuri, A. M., Antonini, G., Ascenzi, P., Nicotra, M., Nuccetelli, M., Mazzetti, A. P., Federici, G., Lo Bello, M., and Ricci, G. (1999) Temperature adaptation of glutathione S-transferase P1-1. A case for homotropic regulation of substrate binding. *J. Biol. Chem. 274*, 19276–19280.
11. Fabrini, R., De Luca, A., Stella, L., Mei, G., Orioni, B., Ciccone, S., Federici, G., Lo Bello, M., and Ricci, G. (2009) Monomer-dimer equilibrium in glutathione transferases: A critical re-examination. *Biochemistry 48*, 10473–10482.
12. Dirr, H. W., and Reinemer, P. (1991) Equilibrium unfolding of class pi glutathione S-transferase. *Biochem. Biophys. Res. Commun. 180*, 294–300.
13. Aceto, A., Caccuri, A. M., Sacchetta, P., Bucciarelli, T., Dragani, B., Rosato, N., Federici, G., and Di Ilio, C. (1992) Dissociation and unfolding of pi-class glutathione transferase. Evidence for a monomeric inactive intermediate. *Biochem. J. 285* (Part 1), 241–245.
14. Erhardt, J., and Dirr, H. (1995) Native dimer stabilizes the subunit tertiary structure of porcine class pi glutathione S-transferase. *Eur. J. Biochem. 230*, 614–620.
15. Kaplan, W., Husler, P., Klump, H., Erhardt, J., Sluis-Cremer, N., and Dirr, H. (1997) Conformational stability of pGEX-expressed *Schistosoma japonicum* glutathione S-transferase: A detoxification enzyme and fusion-protein affinity tag. *Protein Sci. 6*, 399–406.
16. Stevens, J. M., Hornby, J. A., Armstrong, R. N., and Dirr, H. W. (1998) Class sigma glutathione transferase unfolds via a dimeric and a monomeric intermediate: Impact of subunit interface on conformational stability in the superfamily. *Biochemistry 37*, 15534–15541.
17. Wallace, L. A., Sluis-Cremer, N., and Dirr, H. W. (1998) Equilibrium and kinetic unfolding properties of dimeric human glutathione transferase A1-1. *Biochemistry 37*, 5320–5328.
18. Sacchetta, P., Pennelli, A., Bucciarelli, T., Cornelio, L., Amicarelli, F., Miranda, M., and Di Ilio, C. (1999) Multiple unfolded states of glutathione transferase bbGSTP1-1 by guanidinium chloride. *Arch. Biochem. Biophys. 369*, 100–106.
19. Hornby, J. A., Luo, J. K., Stevens, J. M., Wallace, L. A., Kaplan, W., Armstrong, R. N., and Dirr, H. W. (2000) Equilibrium folding of dimeric class mu glutathione transferases involves a stable monomeric intermediate. *Biochemistry 39*, 12336–12344.
20. Lian, H. Y., Jiang, Y., Zhang, H., Jones, G. W., and Perrett, S. (2006) The yeast prion protein Ure2: Structure, function and folding. *Biochim. Biophys. Acta 1764*, 535–545.
21. He, G. J., Zhang, A., Liu, W. F., Cheng, Y., and Yan, Y. B. (2009) Conformational stability and multistate unfolding of poly(A)-specific ribonuclease. *FEBS J. 276*, 2849–2860.
22. Wang, X. Y., Zhang, Z. R., and Perrett, S. (2009) Characterization of the activity and folding of the glutathione transferase from *Escherichia coli* and the roles of residues Cys(10) and His(106). *Biochem. J. 417*, 55–64.
23. Codreanu, S. G., Thompson, L. C., Hachey, D. L., Dirr, H. W., and Armstrong, R. N. (2005) Influence of the dimer interface on glutathione transferase structure and dynamics revealed by amide H/D exchange mass spectrometry. *Biochemistry 44*, 10605–10612.
24. Thompson, L. C., Walters, J., Burke, J., Parsons, J. F., Armstrong, R. N., and Dirr, H. W. (2006) Double mutation at the subunit interface of glutathione transferase rGSTM1-1 results in a stable, folded monomer. *Biochemistry 45*, 2267–2273.
25. Tew, K. D. (1994) Glutathione-associated enzymes in anticancer drug resistance. *Cancer Res. 54*, 4313–4320.
26. Tew, K. D. (2007) Redox in redux: Emergent roles for glutathione S-transferase P (GSTP) in regulation of cell signaling and S-glutathionylation. *Biochem. Pharmacol. 73*, 1257–1269.
27. Adler, V., Yin, Z., Fuchs, S. Y., Benezra, M., Rosario, L., Tew, K. D., Pincus, M. R., Sardana, M., Henderson, C. J., Wolf, C. R., Davis, R. J., and Ronai, Z. (1999) Regulation of JNK signaling by GSTp. *EMBO J. 18*, 1321–1334.
28. Baker, R. T., Smith, S. A., Marano, R., McKee, J., and Board, P. G. (1994) Protein expression using cotranslational fusion and cleavage of ubiquitin. Mutagenesis of the glutathione-binding site of human pi class glutathione S-transferase. *J. Biol. Chem. 269*, 25381–25386.
29. Habig, W. H., and Jakoby, W. B. (1981) Assays for differentiation of glutathione S-transferases. *Methods Enzymol. 77*, 398–405.
30. Pace, C. N., Shirley, B. A., and Thomson, J. A. (1989) Protein structure: A practical approach (Creighton, T. E., Ed.) pp 311−330, IRL Press, Oxford, England.
31. Chamberlain, S. D., Redman, A. M., Wilson, J. W., Deanda, F., Shotwell, J. B., Gerding, R., Lei, H., Yang, B., Stevens, K. L., Hassell, A. M., Shewchuk, L. M., Leesnitzer, M. A., Smith, J. L., Sabbatini, P., Atkins, C., Groy, A., Rowand, J. L., Kumar, R., Mook, R. A., Jr., Moorthy, G., and Patnaik, S. (2009) Optimization of 4,6-bis-anilino-1H-pyrrolo[2,3-d]pyrimidine IGF-1R tyrosine kinase inhibitors towards JNK selectivity. *Bioorg. Med. Chem. Lett. 19*, 360–364.
32. Oakley, A. J., Lo Bello, M., Ricci, G., Federici, G., and Parker, M. W. (1998) Evidence for an induced-fit mechanism operating in pi class glutathione transferases. *Biochemistry 37*, 9912–9917.
33. Chen, R., Li, L., and Weng, Z. (2003) ZDOCK: An initial-stage protein-docking algorithm. *Proteins 52*, 80–87.
34. Pierce, B., and Weng, Z. (2007) ZRANK: Reranking protein docking predictions with an optimized energy function. *Proteins 67*, 1078–1086.
35. Li, L., Chen, R., and Weng, Z. (2003) RDOCK: Refinement of rigid-body protein docking predictions. *Proteins 53*, 693–707.
36. Wang, T., Arifoglu, P., Ronai, Z., and Tew, K. D. (2001) Glutathione S-transferase P1-1 (GSTP1-1) inhibits c-Jun N-terminal kinase (JNK1) signaling through interaction with the C terminus. *J. Biol. Chem. 276*, 20999–21003.
37. Brooks, B. R., Bruccoleri, R. E., Olafson, B. D., States, D. J., Swaminathan, S., and Karplus, M. (1983) CHARMM: A program for macromolecular energy, minimization, and dynamics calculations. *J. Comput. Chem. 4*, 187–217.
38. Reinemer, P., Dirr, H. W., Ladenstein, R., Huber, R., Lo Bello, M., Federici, G., and Parker, M. W. (1992) Three-dimensional structure of class pi glutathione S-transferase from human placenta in complex with S-hexylglutathione at 2.8 Å resolution. *J. Mol. Biol. 227*, 214–226.
39. Dirr, H. W., Little, T., Kuhnert, D. C., and Sayed, Y. (2005) A conserved N-capping motif contributes significantly to the stabilization and dynamics of the C-terminal region of class alpha glutathione S-transferases. *J. Biol. Chem. 280*, 19480–19487.
40. Kinsley, N., Sayed, Y., Mosebi, S., Armstrong, R. N., and Dirr, H. W. (2008) Characterization of the binding of 8-anilinonaphthalene sulfonate to rat class mu GST M1-1. *Biophys. Chem. 137*, 100–104.
41. Abdalla, A. M., and Hamed, R. R. (2006) Multiple unfolding states of glutathione transferase from *Physa acuta* (Gastropoda [correction of Gastropada]: Physidae). *Biochem. Biophys. Res. Commun. 340*, 625–632.
42. Dirr, H. W., and Wallace, L. A. (1999) Role of the C-terminal helix 9 in the stability and ligandin function of class alpha glutathione transferase A1-1. *Biochemistry 38*, 15631–15640.
43. Yassin, Z., Ortiz-Salmeron, E., Garcia-Maroto, F., Baron, C., and Garcia-Fuentes, L. (2004) Implications of the ligandin binding site on the binding of non-substrate ligands to *Schistosoma japonicum* glutathione transferase. *Biochim. Biophys. Acta 1698*, 227–237.
44. Hitchens, T. K., Mannervik, B., and Rule, G. S. (2001) Disorder-to-order transition of the active site of human class pi glutathione transferase, GST P1-1. *Biochemistry 40*, 11660–11669.
45. Ricci, G., Caccuri, A. M., Lo Bello, M., Rosato, N., Mei, G., Nicotra, M., Chiessi, E., Mazzetti, A. P., and Federici, G. (1996) Structural flexibility modulates the activity of human glutathione transferase P1-1. Role of helix 2 flexibility in the catalytic mechanism. *J. Biol. Chem. 271*, 16187–16192.
46. Dirr, H. W., Mann, K., Huber, R., Ladenstein, R., and Reinemer, P. (1991) Class pi glutathione S-transferase from pig lung. Purification,

biochemical characterization, primary structure and crystallization. *Eur. J. Biochem. 196*, 693–698.
47. Ragone, R. (2000) How the protein concentration affects unfolding curves of oligomers. *Biopolymers 53*, 221–225.
48. Rumfeldt, J. A., Galvagnion, C., Vassall, K. A., and Meiering, E. M. (2008) Conformational stability and folding mechanisms of dimeric proteins. *Prog. Biophys. Mol. Biol. 98*, 61–84.
49. Myers, J. K., Pace, C. N., and Scholtz, J. M. (1995) Denaturant m values and heat capacity changes: Relation to changes in accessible surface areas of protein unfolding. *Protein Sci. 4*, 2138–2148.
50. Wallace, L. A., and Matthews, C. R. (2002) Sequential vs. parallel protein-folding mechanisms: Experimental tests for complex folding reactions. *Biophys. Chem. 101−102*, 113–131.
51. Hagerman, P. J., and Baldwin, R. L. (1976) A quantitative treatment of the kinetics of the folding transition of ribonuclease A. *Biochemistry 15*, 1462–1473.
52. Gildenhuys, S., Wallace, L. A., and Dirr, H. W. (2008) Stability and unfolding of reduced *Escherichia coli* glutaredoxin 2: A monomeric structural homologue of the glutathione transferase family. *Biochemistry 47*, 10801–10808.
53. Han, J. H., Batey, S., Nickson, A. A., Teichmann, S. A., and Clarke, J. (2007) The folding and evolution of multidomain proteins. *Nat. Rev. 8*, 319–330.
54. Luo, J. K., Hornby, J. A., Wallace, L. A., Chen, J., Armstrong, R. N., and Dirr, H. W. (2002) Impact of domain interchange on conformational stability and equilibrium folding of chimeric class micro glutathione transferases. *Protein Sci. 11*, 2208–2217.
55. Fanucchi, S., Adamson, R. J., and Dirr, H. W. (2008) Formation of an unfolding intermediate state of soluble chloride intracellular channel protein CLIC1 at acidic pH. *Biochemistry 47*, 11674–11681.
56. Dirr, H., Reinemer, P., and Huber, R. (1994) Refined crystal structure of porcine class pi glutathione S-transferase (pGST P1-1) at 2.1 Å resolution. *J. Mol. Biol. 243*, 72–92.
57. Gunasekaran, K., Eyles, S. J., Hagler, A. T., and Gierasch, L. M. (2001) Keeping it in the family: Folding studies of related proteins. *Curr. Opin. Struct. Biol. 11*, 83–93.
58. Caccuri, A. M., Lo Bello, M., Nuccetelli, M., Nicotra, M., Rossi, P., Antonini, G., Federici, G., and Ricci, G. (1998) Proton release upon glutathione binding to glutathione transferase P1-1: Kinetic analysis of a multistep glutathione binding process. *Biochemistry 37*, 3028–3034.
59. Erhardt, J., and Dirr, H. (1996) Effect of glutathione, glutathione sulphonate and S-hexylglutathione on the conformational stability of class pi glutathione S-transferase. *FEBS Lett. 391*, 313–316.
60. Monaco, R., Friedman, F. K., Hyde, M. J., Chen, J. M., Manolatus, S., Adler, V., Ronai, Z., Koslosky, W., and Pincus, M. R. (1999) Identification of a glutathione-S-transferase effector domain for inhibition of jun kinase, by molecular dynamics. *J. Protein Chem. 18*, 859–866.
61. Ralat, L. A., Manevich, Y., Fisher, A. B., and Colman, R. F. (2006) Direct evidence for the formation of a complex between 1-cysteine peroxiredoxin and glutathione S-transferase pi with activity changes in both enzymes. *Biochemistry 45*, 360–372.
62. Ralat, L. A., Misquitta, S. A., Manevich, Y., Fisher, A. B., and Colman, R. F. (2008) Characterization of the complex of glutathione S-transferase pi and 1-cysteine peroxiredoxin. *Arch. Biochem. Biophys. 474*, 109–118.
63. Manevich, Y., Feinstein, S. I., and Fisher, A. B. (2004) Activation of the antioxidant enzyme 1-CYS peroxiredoxin requires glutathionylation mediated by heterodimerization with pi GST. *Proc. Natl. Acad. Sci. U.S.A. 101*, 3780–3785.